AD-A055 732 PRINCETON UNIV N J DEPT OF CIVIL AND GEOLOGICAL ENG--ETC F/G 20/2
EDGE DISLOCATION IN NONLOCAL HEXAGONAL ELASTIC CRYSTALS.(U)
MAY 78 A C ERINGEN, F BALTA N00014-76-C-0240
UNCLASSIFIED 78-SM-3 NL

| OF |
AD
A055 732

END
DATE
FILMED
8-78
DDC

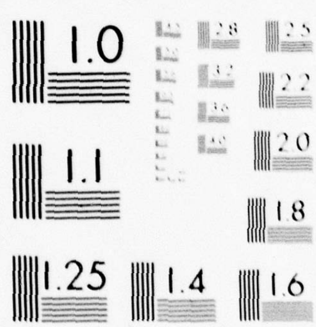

MICROCOPY RESOLUTION TEST CHART

FOR FURTHER TRAN

(12)

AD A055732

DDC FILE COPY

PRINCETON UNIVERSITY

Department of Civil Engineering

STRUCTURES AND MECHANICS

78 06 21 004

Technical Rep. No. ~~52~~ 49
Civil Engng. Res. Rep. No. 78-SM-3

6 EDGE DISLOCATION IN NONLOCAL HEXAGONAL ELASTIC CRYSTALS.

by

9 Technical rept.

10 A. Cemal Eringen
~~and~~
F. Balta

Research Sponsored by the
Office of Naval Research

under

15 Contract N00014-76-C-0240
Modification No. P00002

14 78-SM-3, TR-49

11 May 1978 12 29p.

Approved for Public Release; Distribution Unlimited

EDGE DISLOCATION IN NONLOCAL HEXAGONAL ELASTIC CRYSTALS*

by

A. Cemal Eringen

and

F. Balta

Princeton University

ABSTRACT

The solution is presented for the problems of edge dislocation in hexagonal crystals with long range interatomic interactions. The field equations of nonlocal elastic solids are employed to determine the stress fields and the elastic energy for an edge dislocation in the basal plane. Classical stress and energy singularities are found not present in the nonlocal solutions. Stress distribution is calculated and maximum shear stress is given for various hexagonal materials. Theoretical shear stress to initiate a dislocation having a Burger's vector of one atomic distance is calculated and found to be in the acceptable range known from the lattice dynamic calculations.

1. INTRODUCTION

It is well-known that the classical elasticity solution of the edge dislocation contains stress and energy singularities in the "core region", cf. [1]. In several previous papers (e.g., [2], [3], [4]) we have shown that the solutions of various Volterra dislocations based on the nonlocal elasticity theory do not contain

---

*The present work was supported by the Office of Naval Research

these singularities. This recent theory [5,6] models the elastic materials much more satisfactorily in that the effect of long range interatomic interactions are taken into account. It seems that no artifice such as introducing various atomistic models to estimate the stress and energy in the core region is necessary. Moreover, as a continuum theory all problems can be reduced to boundary-initial value problems.

The discussion of the dislocation problems in anisotropic solids is not a trivial extension even in its classical frame of reference. Moreover because of the orientational effects the state of stress and elastic energy are affected considerably. Consequently the criteria for failure or the generation of dislocations need new investigations. The raison d'être of the present paper stems from these considerations. In Section 2 we present a brief summary of the field equations of the nonlocal elasticity theory. In Section 3 we obtain the solution of the edge dislocation problem leading to stress and energy fields and in Section 4 we specialize these results to the isotropic crystals. In Section 5, some results of computer calculations are presented and maximum stresses that cause a single edge dislocation in several hexagonal crystals (Mg. Apatite, Cd, Zn) are calculated. The distribution of normal and shear stresses along radial line r, $\theta=0$, and as a function of the polar angle θ for a fixed r are calculated. Since no stress and energy singularity occur, the maximum stress hypothesis may be used to calculate the theoretical (cohesive) stress. The results are in the accepted range known from the atomic theory.

2. FORMULATION

In previous papers [2,4] we have shown that, under some very general conditions, the solution of elastostatic problems in linear nonlocal elasticity can be reduced to the solution of the classical Navier's equation, however the stress field is calculated by

$$t_{k\ell}(\underset{\sim}{x}) = \int_V \alpha(\underset{\sim}{x}'-\underset{\sim}{x})\sigma_{k\ell}(\underset{\sim}{x}')dv(\underset{\sim}{x}') \tag{2.1}$$

where $\sigma_{k\ell}$ is given by the classical Hooke's law which for the hexagonal crystals can be arranged into the form, cf. Fig. 1a,

$$\begin{bmatrix} \sigma_{11} \\ \sigma_{22} \\ \sigma_{33} \\ \sigma_{23} \\ \sigma_{31} \\ \sigma_{12} \end{bmatrix} = \begin{bmatrix} C_{11} & C_{12} & C_{13} & & & \\ C_{12} & C_{22} & C_{12} & & & \\ C_{13} & C_{12} & C_{11} & & & \\ & & & 2C_{44} & & \\ & & & & 2C_{55} & \\ & & & & & 2C_{44} \end{bmatrix} \begin{bmatrix} e_{11} \\ e_{22} \\ e_{33} \\ e_{23} \\ e_{31} \\ e_{12} \end{bmatrix} . \tag{2.2}$$

Here $e_{k\ell}$ is the linear strain tensor given by

$$e_{k\ell} \equiv \frac{1}{2}(u_{k,\ell} + u_{\ell,k}) \tag{2.3}$$

where $u_{k,\ell} \equiv \partial u_k/\partial x_\ell$. Since for the hexagonal crystals $2C_{55}=C_{11}-C_{13}$, the number of independent elastic constants are five.

The attenuation function $\alpha(\underset{\sim}{x}'-\underset{\sim}{x})$ suggested in our previous work is of the form

$$(2.4) \qquad \alpha = \alpha_o \exp[-(k_1/a)^2(x'_\beta-x_\beta)(x'_\beta-x_\beta)-(k_2/a)^2(x'_2-x_2)^2]$$

where β is summed over β=1 and β=3. Here a is the lattice parameter k_1 and k_2 are two constants which govern the range of attenuation of the interatomic attractions. The constant α_o is determined from the normalization condition on α:

$$(2.5) \qquad \int_V \alpha(\underset{\sim}{x}'-\underset{\sim}{x})\, dv(\underset{\sim}{x}') = 1$$

so that

$$(2.6) \qquad \alpha_o = k_1^2 k_2/\pi^{3/2}\, a^3 \quad .$$

Now a problem in nonlocal elasticity is reduced to determining the displacement field $u_k(\underset{\sim}{x})$ by solving the Navier's equation obtained by combining (2.2) and (2.3) with the Cauchy's equation

$$(2.7) \qquad \sigma_{k\ell,k} = 0 \quad , \quad k,\ell = 1,2,3$$

where as usual repeated indices are summed over (1,2,3). Once $u_k(\underset{\sim}{x})$ is determined one can then calculate strain from (2.3) and the stress field $t_{k\ell}$ by using (2.2) in (2.1). We now apply this program to solve the problem of the edge dislocations.

3. EDGE DISLOCATION

The straight edge dislocation in a hexagonal crystal is possible in the basal plane y=const. in the x-direction Fig. 1a. We vision such a dislocation by cutting a cylinder along a radial plane and pulling lower surface by a constant amount b (called Burger's vector) relative to the upper surface and welding the two surfaces, Fig. 1b. The solution of this problem in classical elasticity is well-known (cf. [1], p. 422). The displacement field $(u_x, u_y, 0)$ satisfying Navier's equation, is given by

$$(3.1) \qquad u_x = \frac{b}{4\pi} \quad [\arctan (\frac{u_1 xy}{x^2 - \lambda^2 y^2}) + u_2 \ell n(q/t)] \quad ,$$

$$u_y = \frac{-b}{4\pi} \; u_3 \; [u_4 \ell n(qt) - u_5 \arctan (\frac{u_6 y^2}{x^2 - u_7 y^2})]$$

and $\sigma_{k\ell}$ by

$$(3.2) \qquad \sigma_{xx} = -\frac{Mb}{2\pi} \; \frac{\sigma_1 x^2 y + \sigma_2 y^3}{x^4 + p_1 x^2 y^2 + p_2 y^4} \quad ,$$

$$\sigma_{yy} = \frac{Mb}{2\pi} \; \frac{\sigma_3 x^2 y - \sigma_4 y^3}{x^4 + p_1 x^2 y^2 + p_2 y^4} \quad ,$$

$$\sigma_{xy} = \frac{Mb}{2\pi} \; \frac{\sigma_3 x^3 - \sigma_4 x y^2}{x^4 + p_1 x^2 y^2 + p_2 y^4}$$

all other components of $\sigma_{k\ell}$ and u_z vanish. Here we used (x,y,z) for subscripts (1,2,3) and set

$$\bar{C}_{11} \equiv (C_{11}C_{22})^{1/2} \quad , \tag{3.3}$$

$$M \equiv C_{44}(\bar{C}_{11}+C_{12})\{(\bar{C}_{11}-C_{12})/[C_{22}C_{44}(\bar{C}_{11}+C_{12}+2C_{44})]\}^{1/2} \quad ,$$

$$\sigma_1 \equiv [(\bar{C}_{11}-C_{12})(\bar{C}_{11}+C_{12}+2C_{44})-\bar{C}_{11}C_{44}]/(C_{22}C_{44}) \quad ,$$

$$\sigma_2 \equiv C_{11}/C_{22} \quad , \quad \sigma_3 \equiv 1 \quad , \quad \sigma_4 \equiv (C_{11}/C_{22})^{1/2} \quad ,$$

$$p_1 = 2(\bar{C}_{11}/C_{22})+(\bar{C}_{11}+C_{12})(\bar{C}_{11}-C_{12}-2C_{44})/(C_{22}C_{44}) \quad ,$$

$$p_2 \equiv C_{11}/C_{22} \quad ,$$

$$\lambda \equiv (C_{11}/C_{22})^{1/4} \quad , \quad \phi \equiv \frac{1}{2}\arccos[(C_{12}^2+2C_{12}C_{44}-\bar{C}_{11}^2)/(2\bar{C}_{11}C_{44})],$$

$$q^2 \equiv x^2+2\lambda\cos\phi xy+\lambda^2y^2 \quad t^2 \equiv x^2-2\lambda\cos\phi xy+\lambda^2y^2 \quad ,$$

$$u_1 \equiv 2\lambda\sin\phi \quad , \quad u_2 \equiv (\bar{C}_{11}^2-C_{12}^2)/(2\bar{C}_{11}C_{44}\sin 2\phi) \quad ,$$

$$u_3 \equiv \lambda/(\bar{C}_{11}\sin 2\phi) \quad , \quad u_4 \equiv (\bar{C}_{11}-C_{12})\cos\phi \quad ,$$

$$u_5 \equiv (\bar{C}_{11}+C_{12})\sin\phi \quad , \quad u_6 \equiv \lambda^2\sin 2\phi \quad , \quad u_7 \equiv \lambda^2\cos 2\phi$$

Introducing the cylindrical coordinates by (Fig. 2),

$$x = r\cos\theta \quad , \quad y = r\sin\theta \quad , \quad z = z \tag{3.4}$$

$$x' = r'\cos\theta' \quad , \quad y' = r'\sin\theta' \quad , \quad z' = z'$$

$$dv(\underset{\sim}{x}') = r'\,dr'\,d\theta'\,dz'$$

we have for the components of $\sigma_{k\ell}$ in cylindrical coordinates:

$$(3.5)\qquad \sigma_{rr} = \frac{\sigma_{xx}+\sigma_{yy}}{2} + \frac{\sigma_{xx}-\sigma_{yy}}{2}\cos 2\theta + \sigma_{xy}\sin 2\theta \quad ,$$

$$\sigma_{\theta\theta} = \frac{\sigma_{xx}+\sigma_{yy}}{2} - \frac{\sigma_{xx}-\sigma_{yy}}{2}\cos 2\theta - \sigma_{xy}\sin 2\theta \quad ,$$

$$\sigma_{r\theta} = -\frac{\sigma_{xx}-\sigma_{yy}}{2}\sin 2\theta + \sigma_{xy}\cos 2\theta \ .$$

The physical components $t^{(k)}(\ell)$ of the stress tensor in the nonlocal theory are given in terms of those of the classical stresses $\sigma^{(k)}(\ell)$ and shifters $\delta^{k}{}_{k'}$ by

$$(3.6)\qquad t^{(k)}(\ell) = \int_V \alpha(\underset{\sim}{x}'-\underset{\sim}{x})\sigma^{(k')}(\ell')\delta^{\ell'}{}_{\ell}\,\delta^{k}{}_{k'}\,dv(\underset{\sim}{x}')$$

cf. [2]. In cylindrical coordinates the shifters have the following values

$$(3.7)\qquad \delta^{1'}{}_{1} = \delta^{2'}{}_{2} = \underset{\sim}{e}_r\cdot\underset{\sim}{e}'_r = \underset{\sim}{e}_\theta\cdot\underset{\sim}{e}'_\theta = \cos(\theta'-\theta) \quad ,$$

$$\delta^{1'}{}_{2} = \underset{\sim}{e}'_r\cdot\underset{\sim}{e}_\theta = \sin(\theta'-\theta) \quad , \quad \delta^{1}{}_{2'} = \underset{\sim}{e}_r\cdot\underset{\sim}{e}'_\theta = -\sin(\theta'-\theta)$$

$$\delta^{3}{}_{3'} = \underset{\sim}{e}_z\cdot\underset{\sim}{e}'_z = 1 \quad , \quad \delta^{k}{}_{k'} = \delta^{k'}{}_{k} \ .$$

Thus the physical components of the stress tensor have the form

$$(3.8)\quad t_{rr} = \int_V \alpha(\underset{\sim}{x}'-\underset{\sim}{x})\left[\frac{\sigma'_{rr}+\sigma'_{\theta\theta}}{2} + \frac{\sigma'_{rr}-\sigma'_{\theta\theta}}{2}\cos(\theta'-\theta)-\sigma'_{r\theta}\sin2(\theta'-\theta)\right]dv(\underset{\sim}{x}') \quad ,$$

$$t_{\theta\theta} = \int_V \alpha(\underset{\sim}{x}'-\underset{\sim}{x})\left[\frac{\sigma'_{rr}+\sigma'_{\theta\theta}}{2} - \frac{\sigma'_{rr}-\sigma'_{\theta\theta}}{2}\cos(\theta'-\theta)+\sigma'_{r\theta}\sin2(\theta'-\theta)\right]dv(\underset{\sim}{x}') \quad ,$$

$$t_{r\theta} = \int_V \alpha(\underset{\sim}{x}'-\underset{\sim}{x})\left[\frac{\sigma'_{rr}-\sigma'_{\theta\theta}}{2}\sin2(\theta'-\theta)+\sigma'_{r\theta}\cos2(\theta'-\theta)\right]dv(\underset{\sim}{x}') \quad ,$$

where we used the abreviation $\sigma'_{ij} \equiv \sigma_{ij}(\underset{\sim}{x}')$. Using the relations

$$(3.9)\quad \frac{\sigma'_{rr}+\sigma'_{\theta\theta}}{2} = \frac{\sigma'_{xx}+\sigma'_{yy}}{2}\ ,\quad \frac{\sigma'_{rr}-\sigma'_{\theta\theta}}{2} = \frac{\sigma'_{xx}-\sigma'_{yy}}{2}\cos2\theta'+\sigma'_{xy}\sin2\theta'$$

(3.8) may be written as

$$(3.10)\quad t_{rr} = \int_V \alpha(\underset{\sim}{x}'-\underset{\sim}{x})\left[\frac{\sigma'_{xx}+\sigma'_{yy}}{2} + \frac{\sigma'_{xx}-\sigma'_{yy}}{2}\cos2\theta+\sigma'_{xy}\ \sin2\theta\right]dv(\underset{\sim}{x}') \quad ,$$

$$t_{\theta\theta} = \int_V \alpha(\underset{\sim}{x}'-\underset{\sim}{x})\left[\frac{\sigma'_{xx}+\sigma'_{yy}}{2} - \frac{\sigma'_{xx}-\sigma'_{yy}}{2}\cos2\theta-\sigma'_{xy}\sin2\theta\right]dv(\underset{\sim}{x}') \quad ,$$

$$t_{r\theta} = \int_V \alpha(\underset{\sim}{x}'-\underset{\sim}{x})\left[-\frac{\sigma'_{xx}-\sigma'_{yy}}{2}\sin2\theta+\sigma'_{xy}\ \cos2\theta\right]dv(\underset{\sim}{x}') \quad .$$

The attenuation function $\alpha(\underset{\sim}{x}'-\underset{\sim}{x})$ in cylindrical coordinates acquires the form

$$(3.11)\quad \alpha(\underset{\sim}{x}'-\underset{\sim}{x}) = \pi^{-3/2}(k_1^2k_2/a^3)\exp[-(k_1^2/a^2)(z'-z)^2]$$

$$\cdot \exp[-(r^2/a^2)(k_1^2\cos^2\theta+k_2^2\sin^2\theta)]$$

$$\cdot \exp[-(k_1^2/a^2)(r'^2\cos^2\theta'-2rr'\cos\theta\cos\theta')$$

$$-(k_2^2/a^2)(r'^2\sin^2\theta'-2rr'\sin\theta\sin\theta')] \quad .$$

We now substitute (3.4) into (3.2), the result and (3.11) into (3.10). This, for each of the stress components, leads to a triple integral over the domain ($0 \le r' < \infty$, $0 \le \theta' < 2\pi$, $-\infty < z' < \infty$). The integrations over r' and z' are tedious but can be carried out, however the integration over θ' will have to be done numerically. Leaving the details of these calculations we give the results:

$$\{t_{rr}, t_{\theta\theta}, t_{r\theta}\} = \int_0^{2\pi} \{T_{rr}(\theta,\theta'), T_{\theta\theta}(\theta,\theta'), T_{r\theta}(\theta,\theta')\} \cdot f(r,\theta,\theta')d\theta' \tag{3.12}$$

where

$$T_{rr} = -t_o\,(g_1 + g_2 \cos 2\theta - g_3 \sin 2\theta) \tag{3.13}$$

$$T_{\theta\theta} = -t_o\,(g_1 - g_2 \cos 2\theta + g_3 \sin 2\theta)$$

$$T_{r\theta} = t_o\,(g_2 \sin 2\theta + g_3 \cos 2\theta)$$

$$g_1 = q_1 \cos^2\theta' \sin\theta' + q_2 \sin^3\theta' \quad ,$$

$$g_2 = q_3 \cos^2\theta' \sin\theta' + q_4 \sin^3\theta' \quad ,$$

$$g_3 = 2(\sigma_3 \cos^3\theta' - \sigma_4 \cos\theta' \sin^2\theta') \quad ,$$

$$f(r,\theta,\theta') = \frac{\kappa}{4\pi^{1/2}} \exp\{-(kr/a)^2[1+(\kappa^2-1)\sin^2\theta$$

$$-\frac{(\cos\theta\cos\theta'+\kappa^2\sin\theta\sin\theta')^2}{1+(\kappa^2-1)\sin^2\theta'}]\}$$

$$\cdot\{1+\mathrm{erf}[(kr/a)\frac{\cos\theta\cos\theta'+\kappa^2\sin\theta\sin\theta'}{[1+(\kappa^2-1)\sin^2\theta']^{1/2}}]\}$$

$$\cdot(\cos^4\theta'+p_1\sin^2\theta'\cos^2\theta'+p_2\sin^4\theta')^{-1}[1+(\kappa^2-1)\sin^2\theta']^{-1/2}$$

where we also set

$$(3.14)\qquad q_1 \equiv \sigma_1-\sigma_3 \quad , \quad q_2 \equiv \sigma_2+\sigma_4 \quad , \quad q_3 \equiv \sigma_1+\sigma_3 \quad , \quad q_4 \equiv \sigma_2-\sigma_4 \quad ,$$

$$k_1 \equiv k \quad , \quad k_2/k_1 \equiv \kappa \quad , \quad t_o \equiv Mbk/2\pi a \; .$$

The total strain energy is given by

$$(3.15)\qquad \Sigma = 2L \int_0^R\int_0^{\pi/2} (t_{rr}e_{rr}+t_{\theta\theta}e_{\theta\theta}+2t_{r\theta}e_{r\theta})r\;dr\;d\theta$$

where L is the length of the cylinder and R is the radius. Substituting for e_{rr}, $e_{\theta\theta}$ and $e_{r\theta}$ calculated from (2.3), in the same way as in the case for σ_{rr}, $\sigma_{\theta\theta}$, $\sigma_{r\theta}$, we write

$$(3.16)\qquad \Sigma = \frac{MbL}{\pi}\int_0^R\int_0^{\pi/2} [t_{rr}(a_1\cos^4\theta+a_2\cos^2\theta+a_3)\sin\theta+t_{\theta\theta}(a_4\cos^4\theta$$

$$+a_5\cos^2\theta+a_6)\sin\theta+t_{r\theta}(a_7\sin^4\theta+a_8\sin^2\theta+a_9)$$

$$\cos\theta](\cos^4\theta+p_1\sin^2\theta\cos^2\theta+p_2\sin^4\theta)^{-1}d\theta dr$$

where

$$(3.17) \qquad a_1 \equiv (\varepsilon_2-\varepsilon_1)(\sigma_1-\sigma_2)+(\varepsilon_2-\varepsilon_3+\varepsilon_4)(\sigma_3+\sigma_4) \quad ,$$

$$a_2 \equiv -\varepsilon_2\sigma_1+(2\varepsilon_2-\varepsilon_1)\sigma_2+\varepsilon_3\sigma_3+(2\varepsilon_3-\varepsilon_2-\varepsilon_4)\sigma_4 \quad ,$$

$$a_3 \equiv -(\varepsilon_2\sigma_2+\varepsilon_3\sigma_4) \ , \quad a_4 \equiv -a_1 \quad ,$$

$$a_5 \equiv -\varepsilon_1\sigma_1+(2\varepsilon_1-\varepsilon_2)\sigma_2+\varepsilon_2\sigma_3+(2\varepsilon_2-\varepsilon_3+\varepsilon_4)\sigma_4 \quad ,$$

$$a_6 \equiv -(\varepsilon_1\sigma_2+\varepsilon_2\sigma_4) \ , \quad a_7 \equiv 2a_1 \quad ,$$

$$a_8 \equiv 2[(\varepsilon_1-\varepsilon_2)\sigma_1-(\varepsilon_2-\varepsilon_3+\varepsilon_4)\sigma_3]-\varepsilon_4(\sigma_3+\sigma_4) \quad ,$$

$$a_9 \equiv \varepsilon_4\sigma_3 \quad ,$$

and

$$(\varepsilon_1,\varepsilon_2,\varepsilon_3) \equiv (C_{22},-C_{12},C_{11})(C_{11}C_{22}-C_{12}^2)^{-1} \quad , \quad \varepsilon_4 \equiv C_{44}^{-1} \quad .$$

4. ISOTROPIC SOLID

In the case of isotropic solids we have

$$(4.1) \qquad M = \mu/(1-\nu) \ , \ \kappa=1 \ , \ q_1=q_2=2 \ , \ q_3=4 \ , \ q_4=0 \ ,$$

$$\sigma_1=3 \ , \ \sigma_2=\sigma_3=\sigma_4=1 \ , \ p_1=2 \ , \ p_2=1 \ ,$$

$$a_1 = a_2 = a_4 = a_5 = a_7 = a_8 = 0 \quad ,$$

$$a_3 = a_6 = -[2(\lambda+\mu)]^{-1} \quad , \quad a_9 = 1/\mu \quad .$$

Using these values in the expressions of (3.12), (3.13), (3.15) and (3.16) we obtain

$$t_{rr} = -\frac{\mu bk}{2\pi(1-\nu)a}\{1-[1-\exp(-p^2)]p^{-2}\}p^{-1}\sin\theta \quad , \tag{4.2}$$

$$t_{\theta\theta} = \frac{\mu bk}{2\pi(1-\nu)a}\{1-(2+p^{-2})[1-\exp(-p^2)]\}p^{-1}\sin\theta \quad ,$$

$$t_{r\theta} = \frac{\mu bk}{2\pi(1-\nu)a}\{1-[1-\exp(-p^2)]p^{-2}\}p^{-1}\cos\theta \quad ,$$

$$\Sigma = \frac{\mu b^2 L}{16\pi(1-\nu)^2}\{2(1-\nu)[C+\ell n p^2+E_1(p^2)]-1+[1-\exp(-p^2)]p^{-2}\} \quad , \tag{4.3}$$

where C is the Euler's constant and

$$p \equiv kr/a \quad , \quad E_1(x) \equiv \int_x^\infty \frac{e^{-t}}{t}\,dt \quad , \quad C = 0.5772\ldots \quad . \tag{4.4}$$

These results are in complete agreement with those given in [3].

5. DISCUSSION

Components of the stress tensor are plotted in Fig. 3 as a function of the polar angle θ for a fixed radial distance. It is observed that t_{rr} and $t_{\theta\theta}$ have the same shape with their extrema occurring at the same angle. The extremum values of $t_{r\theta}$ differ by an angle $\pi/2$ from those of the normal stresses. For the fracture calculations the state of stress at $\theta=0$ and $\pi/2$ are important. It is known that the cleavage stress

of the crystals is at least twice the maximum shear stress (Kelly [7], p. 17). Of the two state of stress investigated it is found that the one at $\theta=0$ plane is the most important. In Fig. 4 the shear stress is plotted as a function of $p=kr/a$ for a few hexagonal crystals (Zn, Cd, Apatite, Mg). The elastic constants of these materials listed in Table 1 are taken from ref. [8]. The shear stress for an isotropic crystal (with $\nu=0.3$) is also plotted in Fig. 4. The ratio of the shear stress in hexagonal crystals to that of the isotropic solids may be useful from the point of view of technological applications. This is given in Fig. 5 for the same crystals. Finally we give a plot of the elastic energy as a function of the radius of the cylinder, Fig. 6. Of course as the radius of the cylinder R increases the elastic energy also increases. We note however that <u>no singularity is present either in the stress field or in the energy</u>. The usual singularities present in the classical elasticity solutions however appear when the lattice parameter $a \to 0$. This is the classical continuum limit. In Table 1 we give the material moduli, the maximum shear stress and its radial location. The ratio of the attenuation constants κ is taken, by an anology to the wave propagation [10, ch. 6], as $\kappa=2C_{22}/(C_{11}+C_{22})$. In Table 2 the energy ratio of the hexagonal crystals to the isotropic solids is listed for various radii of the cylindrical specimens. Finally, the maximum value of the ratio $t_{r\theta}/C_{44}$ may be used to estimate the theoretical shear strength of the crystal. To compute this we need to estimate the attenuation constant k in $\alpha(\tilde{x}'-\tilde{x})$. This function decreases to its one percent value at n lattice parameter distance if

$$k = 2.146/n \quad .$$

As an example, for zinc we have

$$(kb/a)^{-1}\, t_{r\theta\ max} = 0.197\ 10^{11}\ \text{dyn/cm}^2 \quad .$$

If we choose b=a ([9], p. 516) then

$$t_{r\theta\ max}/C_{44} = \frac{0.197\ 10^{11}}{3.96\ 10^{11}}\ k = 0.050k \quad .$$

The maximum value that Kelly ([7], p. 19) gives

$$t_{r\theta\ max}/C_{44} = 0.034 \quad .$$

Thus by comparing we obtain

$$k = 0.034/0.050 = 0.68 \quad , \quad n = 2.146/0.68 = 3.14 \quad .$$

The maximum values of $t_{r\theta}/C_{44}$ are shown on Table 3 for various hexagonal crystals for n=2, n=2.5 and n=3.0. These results are in the right range as predicted by other methods and atomic considerations. For example, in the atomic theory of crystal lattices it is known that one must take into account the interactions of at least eight closest neighbours to obtain a result consistent with experiments [11, 12]. For hexagonal crystals eighth neighbours corresponds to n=2.

While clearly there is one parameter (namely k) which need be estimated, the range of this parameter can be ascertained from our knowledge in condensed matter. The detail shape of the nonlocal

moduli seems to be less effective so long as it is a candidate to be a distribution. The flexibility in the choice of $\alpha(\underset{\sim}{x}'-\underset{\sim}{x})$ and k should be considered an asset in the sense that for noncrystalline materials and imperfect crystals the attenuation function can be adjusted for a given material once and for all. Afterward all problems for such a solid are reduced to boundary-value problems.

REFERENCES

[1] Hirth, J.P. and Lothe, J. [1968]: Theory of Dislocations, McGraw-Hill.

[2] Eringen, A.C. [1977]: "Screw Dislocation in Nonlocal Elasticity", J. Phys. D: Appl. Phys., Vol. 10, pp. 671-678.

[3] Eringen, A.C. [1977]: "Edge Dislocation in Nonlocal Elasticity", Int. J. Engng. Sci., Vol. 15, pp. 177-183.

[4] Eringen, A.C. and F. Balta [1978]: "Screw Dislocation in Nonlocal Hexagonal Elastic Crystals", scheduled for publication in Crystal Lattice Defects.

[5] Eringen, A.C. [1972]: "Linear Theory of Nonlocal Elasticity and Dispersion of Plane Waves", Int. J. Engng. Sci., 10, 425-435.

[6] Eringen, A.C. [1976]: Continuum Physics, Vol. IV, Acad. Press.

[7] Kelly, A. [1966]: Strong Solids, Oxford.

[8] Hearmon, R.F.S. [1966, 1969]: "The Elastic Constants of Non-Piezoelectric Crystals", Landolf-Börnstein, Numerical Data and Functional Relationships in Science, ed. by Hellwage, K.H., Vols. III/1 and III/2, Springer-Verlag.

[9] Dorn, J.E. and Mitchell, J.B., [1965]: "Slip Mechanism in Single Crystals of Hexagonal Close-Packed Phases", High Strength Materials, ed. by Zackay, V.F., Wiley.

[10] Federov, F.I. [1968]: Elastic Waves in Crystals, Plenum.

[11] Upadhyaya, J.C. and Verma, M.P. [1973]: "Dispersion Relations in some Hexagonal Metals", J. Phys. F: Metal Phys., Vol. 3, p. 640.

[12] Bertoni, C.M., et.al. [1975]: "Three Body Forces in hcp Metals", J. Phys. F: Metal Phys. Vol. 5, p. 419.

Table 1. Maximum Shear Stresses

Material	Elastic Constants $x10^{11} dyn/cm^2$					κ	$t_{r\theta}/t_o$	F_m
	C_{11}	C_{12}	C_{13}	C_{22}	C_{44}			
Zn	16.5	5.0	3.1	6.2	3.96	0.546	0.217	2.30
Mg	5.93	2.14	2.57	6.15	1.64	1.02	0.398	1.45
Cd	11.4	4.00	3.94	5.08	2.00	0.617	0.237	2.05
Apatite	16.7	6.6	1.31	14.0	6.63	0.912	0.389	1.55
Ice(257K)	1.34	0.53	0.65	1.45	0.313	1.04	0.396	1.45

Table 2. Strain Energy Ratio Σ/Σ_o

Material	p=kr/a				
	1.	2.	5.	10.	20.
Isotropic(ν=.3)	0.747	2.000	4.355	6.265	8.199
Isotropic(κ=1 ν=.3)	0.748	2.001	4.354	6.263	8.195
Zn	0.265	0.889	2.751	4.563	6.462
Mg	0.739	1.956	4.204	6.021	7.858
Cd	0.260	0.846	2.456	3.960	5.522
Apatite	0.845	2.338	5.272	7.679	10.121
Ice	0.675	1.777	3.807	5.448	7.107

Table 3. Shear Stress $t_{r\theta}/C_{44}$

Material	n		
	2.0	2.5	3.0
Zn	0.053	0.043	0.036
Mg	0.102	0.082	0.068
Cd	0.071	0.057	0.047
Apatite	0.075	0.060	0.050
Ice	0.112	0.090	0.075

FIGURE CAPTIONS

Figure 1: (a) Hexagonal crystal
(b) Straight edge dislocation

Figure 2: Cylindrical coordinates

Figure 3: Stresses in xy plane versus θ, $p=2.30$.

Figure 4: $t_{r\theta}/t_o$ versus p, $\theta=0$. ($\nu=0.3$ for isotropic case)

Figure 5: $t_{r\theta}/t^o_{r\theta}$, ratio of anisotropic to isotropic shear stress at $\theta=0$. ($\nu=0.3$ for isotropic case)

Figure 6: Σ/Lb^2 versus $p=kR/a$

Table 1: Elastic constants and maximum shear stresses

Table 2: Strain energy ratio Σ/Σ_o

Table 3: Shear stress $t_{r\theta}/C_{44}$

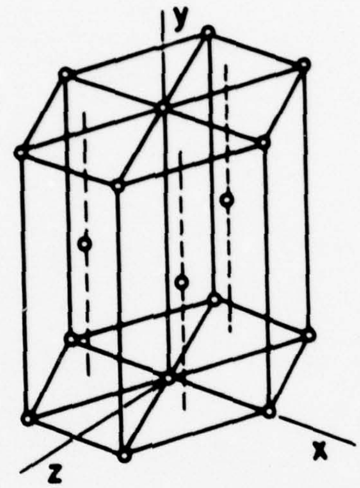

(a)

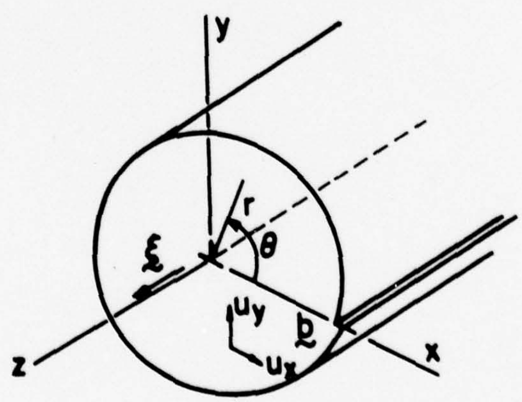

(b)

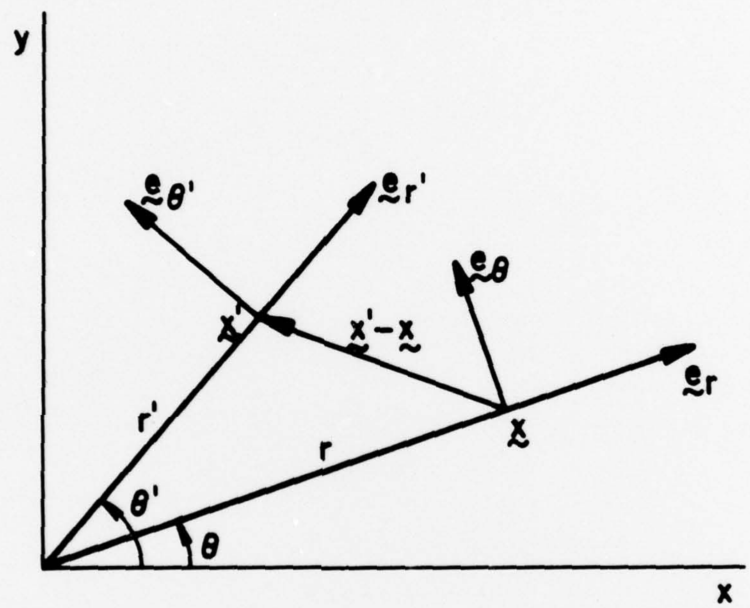
y
$\underset{\sim}{e}_{\theta'}$
$\underset{\sim}{e}_{r'}$
$\underset{\sim}{e}_{\theta}$
$\underset{\sim}{x}'$
$\underset{\sim}{x}'-\underset{\sim}{x}$
$\underset{\sim}{e}_r$
r'
$\underset{\sim}{x}$
r
θ'
θ
x

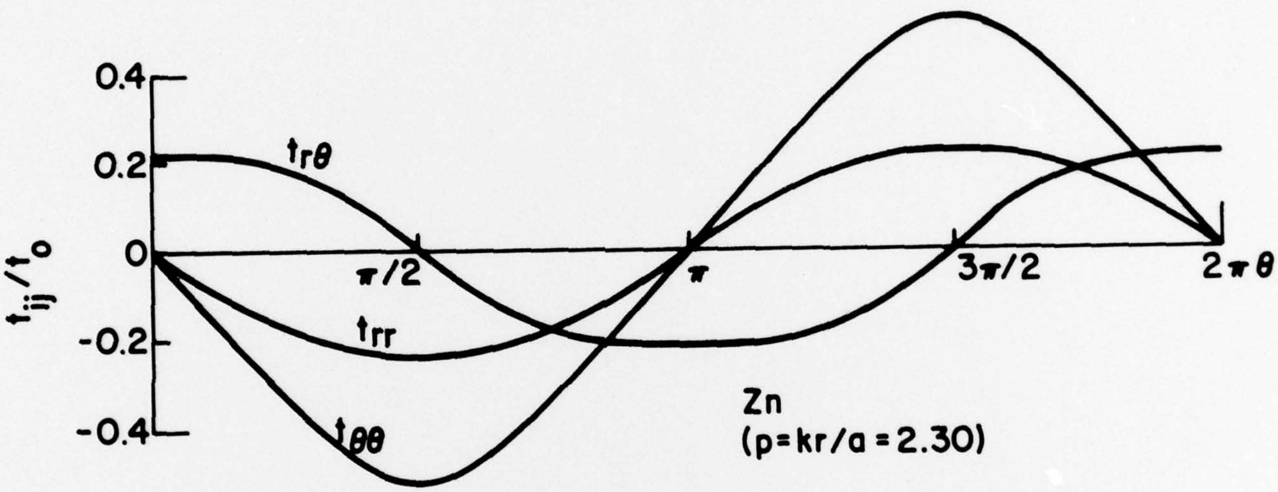

0.4
0.2
0
-0.2
-0.4
t_{ij}/t_o
$t_{r\theta}$
t_{rr}
$t_{\theta\theta}$
$\pi/2$
π
$3\pi/2$
$2\pi\ \theta$
Zn
(p=kr/a=2.30)

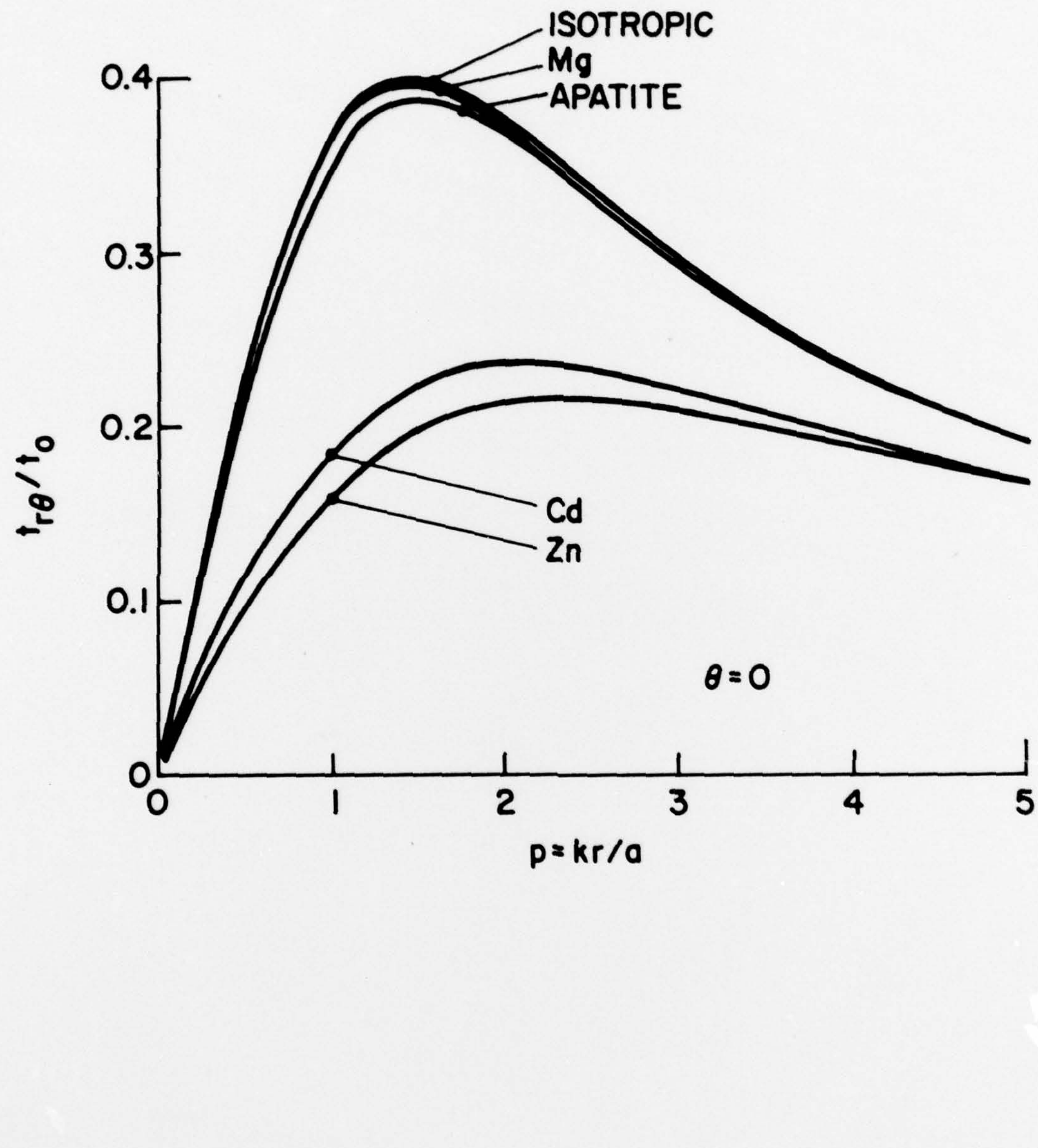
ISOTROPIC
Mg
APATITE
Cd
Zn
$\theta = 0$
$t_{r\theta}/t_o$
$p = kr/a$
0
0.1
0.2
0.3
0.4
0
1
2
3
4
5

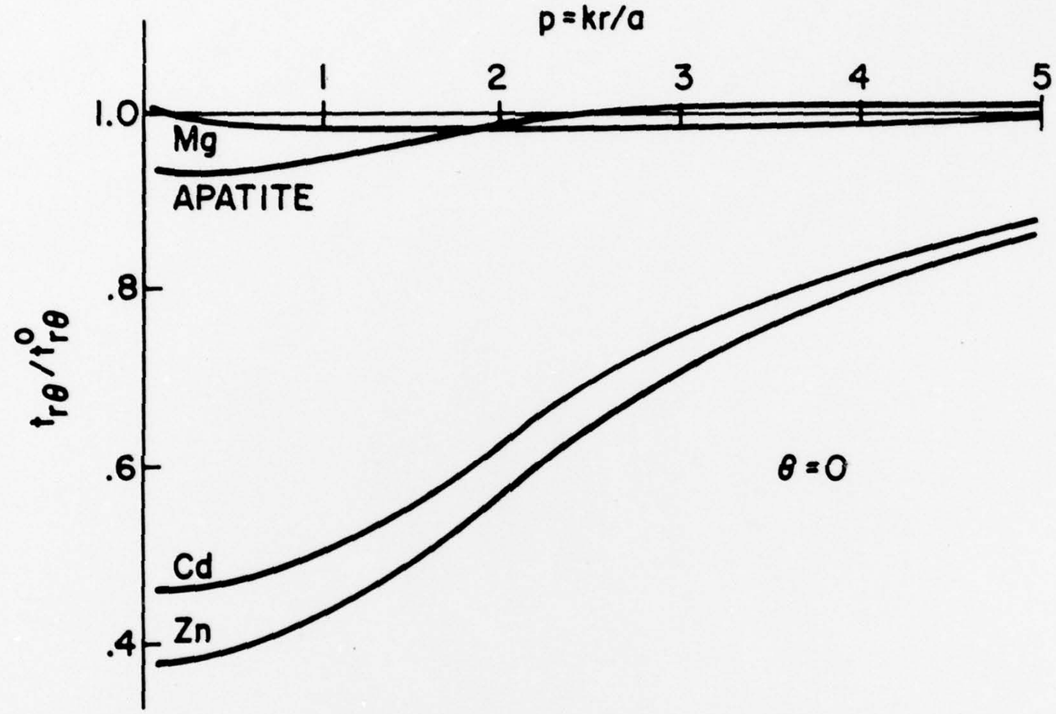

p = kr/a
1
2
3
4
5
1.0
.8
.6
.4
Mg
APATITE
Cd
Zn
$t_{r\theta}/t^o_{r\theta}$
θ = 0

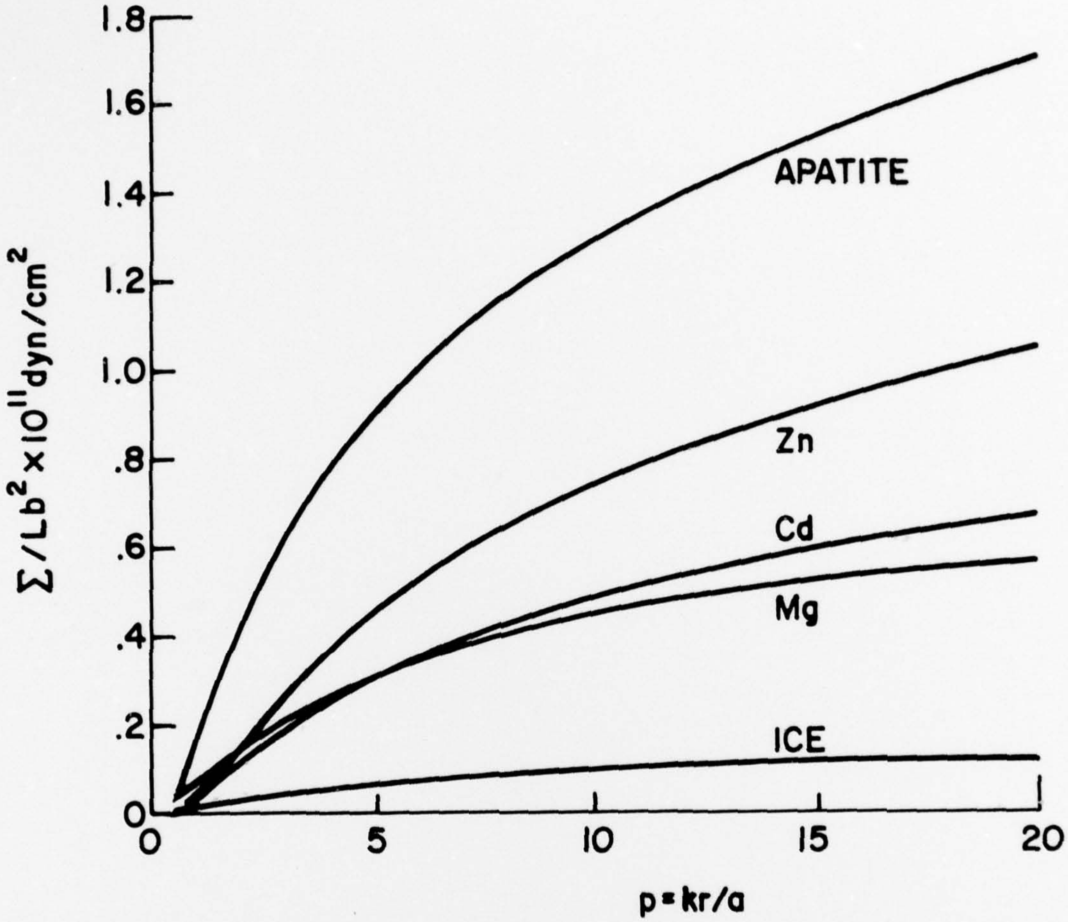

1.8
1.6
1.4
1.2
1.0
.8
.6
.4
.2
0
$\Sigma/Lb^2 \times 10^{11} dyn/cm^2$
APATITE
Zn
Cd
Mg
ICE
0
5
10
15
20
p = kr/a

SECURITY CLASSIFICATION OF THIS PAGE (When Data Entered)

REPORT DOCUMENTATION PAGE

READ INSTRUCTIONS BEFORE COMPLETING FORM

1. REPORT NUMBER: Technical Report 49	2. GOVT ACCESSION NO.
3. RECIPIENT'S CATALOG NUMBER	
4. TITLE (and Subtitle): Edge Dislocation in Nonlocal Hexagonal Elastic Crystals	5. TYPE OF REPORT & PERIOD COVERED: Technical Report
	6. PERFORMING ORG. REPORT NUMBER
7. AUTHOR(s): A. C. Eringen and F. Balta	8. CONTRACT OR GRANT NUMBER(s): N00014-76-C-0240
9. PERFORMING ORGANIZATION NAME AND ADDRESS: Princeton University, Princeton, NJ 08540	10. PROGRAM ELEMENT, PROJECT, TASK AREA & WORK UNIT NUMBERS: P00002
11. CONTROLLING OFFICE NAME AND ADDRESS: Office of Naval Research (Code 471), Arlington, VA 22217	12. REPORT DATE: May 1978
	13. NUMBER OF PAGES: 25
14. MONITORING AGENCY NAME & ADDRESS (if different from Controlling Office)	15. SECURITY CLASS. (of this report): Unclassified
	15a. DECLASSIFICATION/DOWNGRADING SCHEDULE

16. DISTRIBUTION STATEMENT (of this Report)

Approved for public release; Distribution Unlimited

17. DISTRIBUTION STATEMENT (of the abstract entered in Block 20, if different from Report)

18. SUPPLEMENTARY NOTES

19. KEY WORDS (Continue on reverse side if necessary and identify by block number)

edge dislocation, hexagonal crystals, fracture, nonlocal continuum mechanics

20. ABSTRACT (Continue on reverse side if necessary and identify by block number)

The solution is presented for the problems of edge dislocation in hexagonal crystals with long range interatomic interactions. The field equations of non-local elastic solids are employed to determine the stress fields and the elastic energy for an edge dislocation in the basal plane. Classical stress and energy singularities are found not present in the nonlocal solutions. Stress distribution is calculated and maximum shear stress is given for various hexagonal materials. Theoretical shear stress to initiate a dislocation having a Burger's vector of one atomic distance is calculated and found to be in the

next page

20. acceptable range known from the lattice dynamic calculations.

PART 1 - GOVERNMENT

Administrative & Liaison Activities

Chief of Naval Research
Department of the Navy
Arlingon, Virginia 22217
Attn: Code 474 (2)
471
222

Director
ONR Branch Office
495 Summer Street
Boston, Massachusetts 02210

Director
ONR Branch Office
219 S. Dearborn Street
Chicago, Illinois 60604

Director
Naval Research Laboratory
Attn: Code 2629 (ONRL)
Washington, D.C. 20390 (6)

U.S. Naval Research Laboratory
Attn: Code 2627
Washington, D.C. 20390

Director
ONR - New York Area Office
715 Broadway - 5th Floor
New York, N.Y. 10003

Director
ONR Branch Office
1030 E. Green Street
Pasadena, California 91101

Defense Documentation Center
Cameron Station
Alexandria, Virginia 22314 (12)

Army

Commanding Officer
U.S. Army Research Office Durham
Attn: Mr. J. J. Murray
CRD-AA-IP
Box CM, Duke Station
Durham, North Carolina 27706

Commanding Officer
AMXMR-ATL
Attn: Mr. R. Shea
U.S. Army Materials Res. Agency
Watertown, Massachusetts 02172

Watervliet Arsenal
MAGGS Research Center
Watervliet, New York 12189
Attn: Director of Research

Technical Library

Redstone Scientific Info. Center
Chief, Document Section
U.S. Army Missile Command
Redstone Arsenal, Alabama 35809

Army R&D Center
Fort Belvoir, Virginia 22060

Navy

Commanding Officer and Director
Naval Ship Research & Development Center
Bethesda, Maryland 20034
Attn: Code 042 (Tech. Lib. Br.)
17 (Struc. Mech. Lab.)
172
172
174
177
1800 (Appl. Math. Lab.)
5412S (Dr. W.D. Sette)
19 (Dr. M.M. Sevik)
1901 (Dr. M. Strassberg)
1945
196 (Dr. D Feit)
1962

Naval Weapons Laboratory
Dahlgren, Virginia 22448

Naval Research Laboratory
Washington, D.C. 20375
Attn: Code 8400
8410
8430
8440
6300
6390
6380

Undersea Explosion Research Div.
Naval Ship R&D Center
Norfolk Naval Shipyard
Portsmouth, Virginia 23709
Attn: Dr. E. Palmer
Code 780

Naval Ship Research & Development Center
Annapolis Division
Annapolis, Maryland 21402
Attn: Code 2740 - Dr. Y.F. Wang
28 - Mr. R.J. Wolfe
281 - Mr. R.B. Niederberger
2814 - Dr. H. Vanderveldt

Technical Library
Naval Underwater Weapons Center
Pasadena Annex
3202 E. Foothill Blvd.
Pasadena, California 91107

U.S. Naval Weapons Center
China Lake, California 93557
Attn: Code 4062 - Mr. W. Werback
4520 - Mr. Ken Bischel

Commanding Officer
U.S. Naval Civil Engr. Lab.
Code L31
Port Hueneme, California 93041

Technical Director
U.S. Naval Ordnance Laboratory
White Oak
Silver Spring, Maryland 20910

Technical Director
Naval Undersea R&D Center
San Diego, California 92132

Supervisor of Shipbuilding
U.S. Navy
Newport News, Virginia 23607

Technical Director
Mare Island Naval Shipyard
Vallejo, California 94592

U.S. Navy Underwater Sound Ref. Lab.
Office of Naval Research
P.O. Box 8337
Orlando, Florida 32806

Chief of Naval Operations
Dept. of the Navy
Washington, D.C. 20350
Attn: Code Op07T

Strategic Systems Project Office
Department of the Navy
Washington, D.C. 20390
Attn: NSP-001 Chief Scientist

Deep Submergence Systems
Naval Ship Systems Command
Code 39522
Department of the Navy
Washington, D.C. 20360

Engineering Dept.
U.S. Naval Academy
Annapolis, Maryland 21402

Naval Air Systems Command
Dept. of the Navy
Washington, D.C. 20360
Attn: NAVAIR 5302 Aero & Structures
5308 Structures
52031F Materials
604 Tech. Library
320B Structures

Director, Aero Mechanics
Naval Air Development Center
Johnsville
Warminster, Pennsylvania 18974

Technical Director
U.S. Naval Undersea R&D Center
San Diego, California 92132

Engineering Department
U.S. Naval Academy
Annapolis, Maryland 21402

Naval Facilities Engineering Command
Dept. of the Navy
Washington, D.C. 20360
Attn: NAVFAC 03 Research & Development
04 " "
14114 Tech. Library

Naval Sea Systems Command
Dept. of the Navy
Washington, D.C. 20360
Attn: NAVSHIP 03 Res. & Technology
031 Ch. Scientist for R
03412 Hydromechanics
037 Ship Silencing Div.
035 Weapons Dynamics

Naval Ship Engineering Center
Prince George's Plaza
Hyattsville, Maryland 20782
Attn: NAVSEC 6100 Ship Sys Engr & Des Dep
6102C Computer-Aided Ship Des
6105G
6110 Ship Concept Design
6120 Hull Div.
6120D Hull Div.
6128 Surface Ship Struct.
6129 Submarine Struct.

Air Force

Commander WADD
Wright-Patterson Air Force Base
Dayton, Ohio 45433
Attn: Code WWRMDD
AFFDL (FDDS)
Structures Division
AFLC (MCEEA)

Chief, Applied Mechanics Group
U.S. Air Force Inst. of Tech.
Wright-Patterson Air Force Base
Dayton, Ohio 45433

Chief, Civil Engineering Branch
WLRC, Research Division
Air Force Weapons Laboratory
Kirtland AFB, New Mexico 87117

Air Force Office of Scientific Research
1400 Wilson Blvd.
Arlington, Virginia 22209
Attn: Mechanics Div.

NASA

Structures Research Division
National Aeronautics & Space Admin.
Langley Research Center
Langley Station
Hampton, Virginia 23365

National Aeronautic & Space Admin.
Associate Administrator for Advanced
Research & Technology
Washington, D.C. 02546

Scientific & Tech. Info. Facility
NASA Representative (S-AK/DL)
P.O. Box 5700
Bethesda, Maryland 20014

Other Government Activities

Commandant
Chief, Testing & Development Div.
U.S. Coast Guard
1300 E. Street, N.W.
Washington, D.C. 20226

Technical Director
Marine Corps Dev. & Educ. Command
Quantico, Virginia 22134

Director
National Bureau of Standards
Washington, D.C. 20234
Attn: Mr. B.L. Wilson, EM 219

Dr. M. Gaus
National Science Foundation
Engineering Division
Washington, D.C. 20550

Science & Tech. Division
Library of Congress
Washington, D.C. 20540

Director
Defense Nuclear Agency
Washington, D.C. 20305
Attn: SPSS

Commander Field Command
Defense Nuclear Agency
Sandia Base
Albuquerque, New Mexico 87115

Director Defense Research & Engrg
Technical Library
Room 3C-128
The Pentagon
Washington, D.C. 20301

Chief, Airframe & Equipment Branch
FS-120
Office of Flight Standards
Federal Avaiation Agency
Washington, D.C. 20553

Chief, Research and Development
Maritime Administration
Washington, D.C. 20235

Deputy Chief, Office of Ship Constr.
Maritime Administration
WASH. DC 20235
Attn. Mr. U. L. Russo

Atomic Energy Commission
Div. of Reactor Devel. & Tech.
Germantown, Maryland 20767

Ship Hull Research Committee
National Research Council
National Academy of Sciences
2101 Constitution Avenue
Washington, D.C. 20418
Attn: Mr. A.R. Lytle

- - - - -

PART 2 - CONTRACTORS AND OTHER TECHNICAL COLLABORATORS

- - - - -

Universities

Dr. J. Tinsley Oden
University of Texas at Austin
345 Eng. Science Bldg.
Austin, Texas 78712

Prof. Julius Miklowitz
California Institute of Technology
Div. of Engineering & Applied Sciences
Pasadena, California 91109

Dr. Harold Liebowitz, Dean
School of Engr. & Applied Science
George Washington University
725 - 23rd St., N.W.
Washington, D.C. 20006

Prof. Eli Sternberg
California Institute of Technology
Div. of Engr. & Applied Sciences
Pasadena, California 91109

Prof. Paul M. Naghdi
University of California
Div. of Applied Mechanics
Etcheverry Hall
Berkeley, California 94720

Professor P. S. Symonds
Brown University
Division of Engineering
Providnece, R.I. 02912

Prof. A. J. Durelli
The Catholic University of America
Civil/Mechanical Engineering
Washington, D.C. 20017

Prof. R.B. Testa
Columbia University
Dept. of Civil Engineering
S.W. Mudd Bldg.
New York, N.Y. 10027

Prof. H. H. Bleich
Columbia University
Dept. of Civil Engineering
Amsterdam & 120th St.
New York, N.Y. 10027

Prof. F.L. DiMaggio
Columbia University
Dept. of Civil Engineering
616 Mudd Building
New York, N.Y. 10027

Prof. A.M. Freudenthal
George Washington University
School of Engineering & Applied Science
Washington, D.C. 20006

D. C. Evans
University of Utah
Computer Science Division
Salt Lake City, Wash 84112

Prof. Norman Jones
Massachusetts Inst. of Technology
Dept. of Naval Architecture & Marine Engrng
Cambridge, Massachusetts 02139

Professor Albert I. King
Biomechanics Research Center
Wayne State University
Detroit, Michigan 48202

Dr. V. R. Hodgson
Wayne State University
School of Medicine
Detroit, Michigan 48202

Dean B. A. Boley
Northwestern University
Technological Institute
2145 Sheridan Road
Evanston, Illinois 60201

Prof. P.G. Hodge, Jr.
University of Minnesota
Dept. of Aerospace Engng & Mechanics
Minneapolis, Minnesota 55455

Dr. D.C. Drucker
University of Illinois
Dean of Engineering
Urbana, Illinois 61801

Prof. N.M. Newmark
University of Illinois
Dept. of Civil Engineering
Urbana, Illinois 61801

Prof. E. Reissner
University of California, San Diego
Dept. of Applied Mechanics
La Jolla, California 92037

Prof. William A. Nash
University of Massachusetts
Dept. of Mechanics & Aerospace Engng.
Amherst, Massachusetts 01002

Library (Code 0384)
U.S. Naval Postgraduate School
Monterey, California 93940

Prof. Arnold Allentuch
Newark College of Engineering
Dept. of Mechanical Engineering
323 High Street
Newark, New Jersey 07102

Dr. George Herrmann
Stanford University
Dept. of Applied Mechanics
Stanford, California 94305

Prof. J. D. Achenbach
Northwestern University
Dept. of Civil Engineering
Evanston, Illinois 60201

Director, Applied Research Lab.
Pennsylvania State University
P. O. Box 30
State College, Pennsylvania 16801

Prof. Eugen J. Skudrzyk
Pennsylvania State University
Applied Research Laboratory
Dept. of Physics - P.O. Box 30
State College, Pennsylvania 16801

Prof. J. Kempner
Polytechnic Institute of Brooklyn
Dept. of Aero.Engrg.& Applied Mech
333 Jay Street
Brooklyn, N.Y. 11201

Prof. J. Klosner
Polytechnic Institute of Brooklyn
Dept. of Aerospace & Appl. Mech.
333 Jay Street
Brooklyn, N.Y. 11201

Prof. R.A. Schapery
Texas A&M University
Dept. of Civil Engineering
College Station, Texas 77840

Prof. W.D. Pilkey
University of Virginia
Dept. of Aerospace Engineering
Charlottesville, Virginia 22903

Dr. H.G. Schaeffer
University of Maryland
Aerospace Engineering Dept.
College Park, Maryland 20742

Prof. K.D. Willmert
Clarkson College of Technology
Dept. of Mechanical Engineering
Potsdam, N.Y. 13676

Dr. J.A. Stricklin
Texas A&M University
Aerospace Engineering Dept.
College Station, Texas 77843

Dr. L.A. Schmit
University of California, LA
School of Engineering & Applied Science
Los Angeles, California 90024

Dr. H.A. Kamel
The University of Arizona
Aerospace & Mech. Engineering Dept.
Tucson, Arizona 85721

Dr. B.S. Berger
University of Maryland
Dept. of Mechanical Engineering
College Park, Maryland 20742

Prof. G. R. Irwin
Dept. of Mechanical Engrg.
University of Maryland
College Park, Maryland 20742

Dr. S.J. Fenves
Carnegie-Mellon University
Dept. of Civil Engineering
Schenley Park
Pittsburgh, Pennsylvania 15213

Dr. Ronald L. Huston
Dept. of Engineering Analysis
Mail Box 112
University of Cincinnati
Cincinnati, Ohio 45221

Prof. George Sih
Dept. of Mechanics
Lehigh University
Bethlehem, Pennsylvania 18015

Prof. A.S. Kobayashi
University of Washington
Dept. of Mechanical Engineering
Seattle, Washington 98105

Librarian
Webb Institute of Naval Architecture
Crescent Beach Road, Glen Cove
Long Island, New York 11542

Prof. Daniel Frederick
Virginia Polytechnic Institute
Dept. of Engineering Mechanics
Blacksburg, Virginia 24061

Prof. A.C. Eringen
Dept. of Aerospace & Mech. Sciences
Princeton University
Princeton, New Jersey 08540

Dr. S.L. Koh
School of Aero., Astro.& Engr. Sc.
Purdue University
Lafayette, Indiana 47907

Prof. E.H. Lee
Div. of Engrg. Mechanics
Stanford University
Stanford, California 94305

Prof. R.D. Mindlin
Dept. of Civil Engrg.
Columbia University
S.W. Mudd Building
New York, N.Y. 10027

Prof. S.B. Dong
University of California
Dept. of Mechanics
Los Angeles, California 90024

Prof. Burt Paul
University of Pennsylvania
Towne School of Civil & Mech. Engrg.
Rm. 113 - Towne Building
220 S. 33rd Street
Philadelphia, Pennsylvania 19104

Prof. H.W. Liu
Dept. of Chemical Engr. & Metal.
Syracuse University
Syracuse, N.Y. 13210

Prof. S. Bodner
Technion R&D Foundation
Haifa, Israel

Prof. R.J.H. Bollard
Chairman, Aeronautical Engr. Dept.
207 Guggenheim Hall
University of Washington
Seattle, Washington 98105

Prof. G.S. Heller
Division of Engineering
Brown University
Providence, Rhode Island 02912

Prof. Werner Goldsmith
Dept. of Mechanical Engineering
Div. of Applied Mechanics
University of California
Berkeley, California 94720

Prof. J.R.Rice
Division of Engineering
Brown University
Providence, Rhode Island 02912

Prof. R.S. Rivlin
Center for the Application of Mathematics
Lehigh University
Bethlehem, Pennsylvania 18015

Library (Code 0384)
U.S. Naval Postgraduate School
Monterey, California 93940

Dr. Francis Cozzarelli
Div. of Interdisciplinary
Studies & Research
School of Engineering
State University of New York
Buffalo, N.Y. 14214

Industry and Research Institutes

Library Services Department
Report Section Bldg. 14-14
Argonne National Laboratory
9700 S. Cass Avenue
Argonne, Illinois 60440

Dr. M. C. Junger
Cambridge Acoustical Associates
129 Mount Auburn St.
Cambridge, Massachusetts 02138

Dr. L.H. Chen
General Dynamics Corporation
Electric Boat Division
Groton, Connecticut 06340

Dr. J.E. Greenspon
J.G. Engineering Research Associates
3831 Menlo Drive
Baltimore, Maryland 21215

Dr. S. Batdorf
The Aerospace Corp.
P.O. Box 92957
Los Angeles, California 90009

Dr. K.C. Park
Lockheed Palo Alto Research Laboratory
Dept. 5233, Bldg. 205
3251 Hanover Street
Palo Alto, CA 94304

Library
Newport News Shipbuilding &
Dry Dock Company
Newport News, Virginia 23607

Dr. W.F. Bozich
McDonnell Douglas Corporation
5301 Bolsa Ave.
Huntington Beach, CA 92647

Dr. H.N. Abramson
Southwest Research Institute
Technical Vice President
Mechanical Sciences
P.O. Drawer 28510
San Antonio, Texas 78284

Dr. R.C. DeHart
Southwest Research Institute
Dept. of Structural Research
P.O. Drawer 28510
San Antonio, Texas 78284

Dr. M.L. Baron
Weidlinger Associates,
Consulting Engineers
110 East 59th Street
New York, N.Y. 10022

Dr. W.A. von Riesemann
Sandia Laboratories
Sandia Base
Albúquerque, Ney Mexico 87115

Dr. T.L. Geers
Lockheed Missiles & Space Co.
Palo Alto Research Laboratory
3251 Hanover Street
Palo Alto, California 94304

Dr. J.L. Tocher
Boeing Computer Services, Inc.
P.O. Box 24346
Seattle, Washington 98124

Mr. Willian Caywood
Code BBE, Applied Physics Laboratory
8621 Georgia Avenue
Silver Spring, Maryland 20034

Mr. P.C. Durup
Lockheed-California Company
Aeromechanics Dept., 74-43
Burbank, California 91503